TAO, Vol. 7, No. 4, 409-429, December 1996

Q_p Structure in the Taiwan Area and Its Correlation to Seismicity

Kuang-Jung Chen[1], Yih-Hsiung Yeh[2], and Chuen-Tien Shyu[3]

(Manuscript received 7 February 1996, in final form 5 November 1996)

ABSTRACT

The seismic waveform data recorded by the Taiwan Telemetered Seismographic Network (TTSN) were used to deduce the three-dimensional Q_p structure beneath Taiwan. The data consist of three-dimensional, digital seismograms of 98 earthquakes with magnitudes between 2.2 and 5.7. The Q_p structure was obtained by the damped least-square method from attenuation time values (t^*) and travel times. Attenuation time values (t^*) were calculated from these events by using a spectral decay technique under the assumption of that t^* is independent of frequency. P-wave spectra were corrected for a source spectrum of ω^2 model. Least-square fitting was done in the frequency domain of 4 to 25 Hz. Frequencies above 25 Hz are usually avoided due to the uncertainty of instrument correction. Our results show that the distribution pattern of Q_p values in the Taiwan area correlate well with the seismicity. In the upper crust (depths of between 0 to 10 km), the lower Q_p area is consistent with an area of higher seismicity. However, in the lower crust (10 to 25 km) and upper mantle, the area of higher seismicity is consistent with higher Q_p values.

(Key words: Q_p structure, Attenuation time values, Seismicity)

1. INTRODUCTION

The tectonic features of the Taiwan area is extremely complicated because of the nearby convergence of the Eurasian and Philippine Sea plates. The collision of the Philippine Sea and Eurasian plates together with the spreading of the Okinawa Trough, are the main reasons for the complex geological structures and high seismicity in this region (Figure 1). Recently, Roecker *et al.* (1987) applied a three-dimensional block inversion method to obtain the velocity structure of this area, and reported the existence of velocity heterogeneity in the uppermost mantle. It is believed that the high-velocity zones are generally associated with the subducted Philippine Sea plate. However, the corresponding attenuative properties beneath this region have not yet been investigated to a sufficient resolution.

[1]Department of Earth Sciences, National Taiwan Normal University, Taipei, Taiwan, R.O.C.
[2]Institute of Earth Sciences, Academia Sinica, P. O. Box 1-55, Nankang, Taipei, Taiwan, R.O.C.
[3]Institute of Oceanography, National Taiwan University, Taipei, Taiwan, R.O.C.

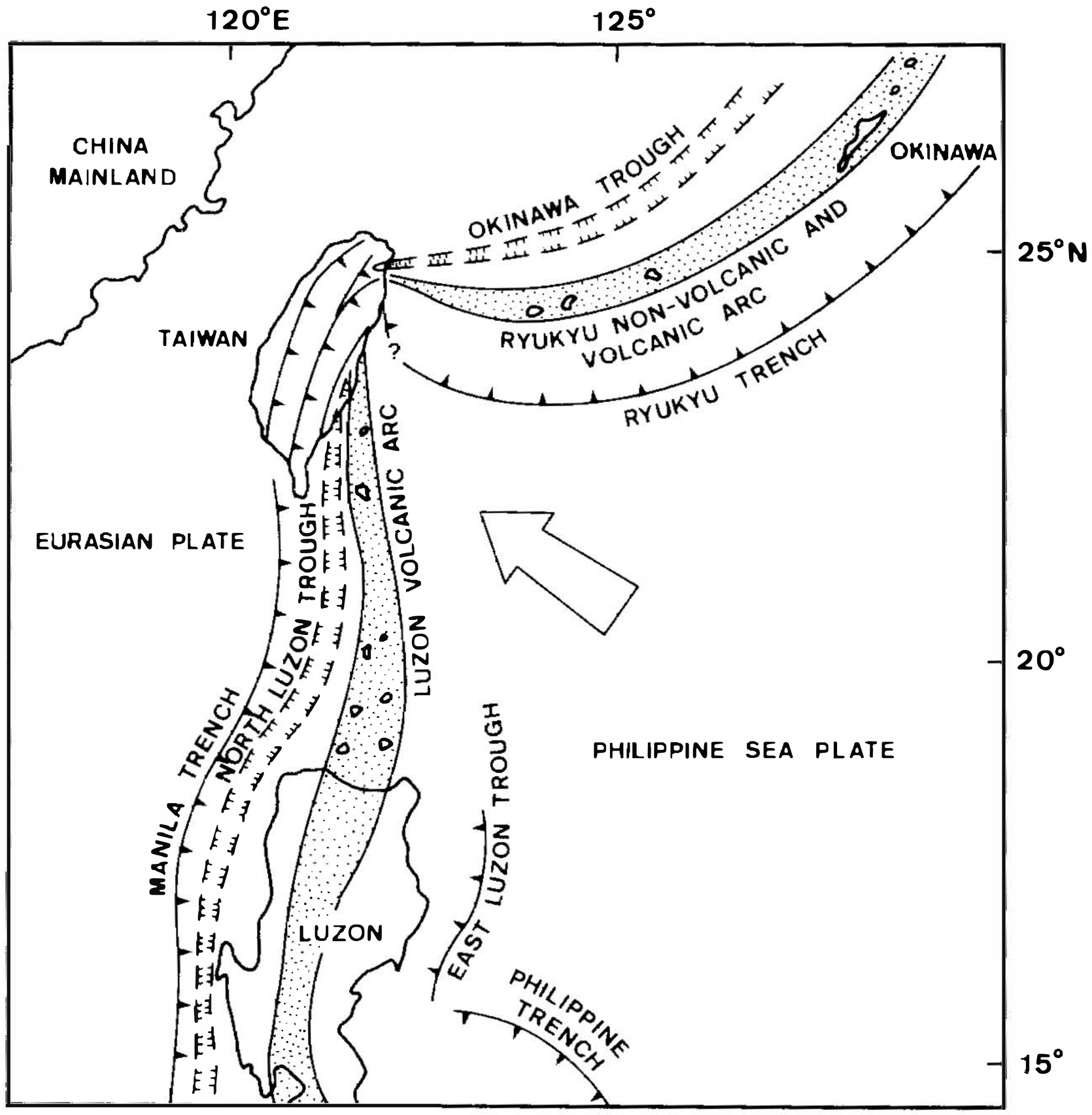

Fig. 1. Regional plate tectonic setting of Taiwan and the neighboring region (after Ho, 1986), showing the interaction of the Philippine Sea and Eurasian plates in Taiwan with the Ryukyu arc system developing to the east and northeast, and Luzon arc system extending to the south.

Attenuation of seismic energy is an important seismic parameter that is not well understood and is difficult to measure. Measurement of this parameter is essential for the prediction of ground motion produced by earthquakes or explosions, for the determination of earthquake magnitude, for the understanding of regional geodynamics, and for the evaluation of seismic risk. Attenuation estimates are also very useful in characterizing certain physical properties of rock materials that cannot be inferred from seismic velocities.

Studies on the attenuation of seismic waves have occupied a significant portion of seismic literature over the years (Der and McElfresh, 1976; Al-Shunkri *et al.*, 1988; Kanamori, 1967; 1967a; 1967b; Lee and Solomon,1978; Solomon, 1972; 1973; Teng, 1968). Attenuation measurements can carry much information regarding the physical state of the Earth's interior and are important in making corrections for source mechanism studies. Observations of lateral variations in Q may aid in determining regional differences in temperature, phase, and composition.

In the present study, we use seismic data collected by the TTSN to obtain a 3-dimen sional model of the Q_p structure for the Taiwan area, since the Q_p structure can provide useful information for an understanding of the tectonics, and for inferences on the temperature distribution in the upper mantle. For this purpose, we have used spectral decay of seismic P phase as the basic observed data. The region to be studied is divided into many blocks, in which the Q_p value is assumed to be constant. The Q_p values in these blocks are estimated as an inverse problem from the observed data.

2. SPECTRAL DECAY METHOD

Q is a dimensionless quantity that measures the amount of energy dissipated per radian as seismic waves propogate. In other words, a seismic wave loses $1/Q$ of its energy after traveling each radian due to the anelasticity of the media. Laboratory studies have shown Q to be independent of frequency (Knopoff, 1964). However, theoretically, Q varies significantly as a function of frequency for a material of uniform composition and grain size (Hough and Anderson, 1988). Also, in a composite viscoelastic material model with a range of relaxation times, Q varies smoothly with frequency and may be considered to be constant over a narrow frequency band (Kanamori and Anderson, 1977). The basic assumption that Q is independent of frequency within the interested frequency band is often made in studies of seismic wave attenuation using the reduced spectral ratio technique (Teng, 1968; Solomon, 1972, 1973).

The effect of Q on a seismic ray describes the time variation of the displacement spectrum $A(r,f)$, i.e.

$$A(r,f)=A_0(r,f)e^{-\pi f t^*} \tag{1}$$

where

$$t^* = \int_0^t \frac{dr}{QV} \tag{2}$$

in which V is the wave velocity, Q is the spatial attenuation factor, and the integral is along the ray path (Kanamori, 1967). The spectrum of displacement, observed at a site distance r from the epicenter, $A(r, f)$ may be approximated by

$$A(r, f)= (2\pi f)^2 S(f)G(r, f)e^{-\pi f t^*} \tag{3}$$

where $G(r, f)$ gives the effect of geometrical spreading that is usually assumed to be independent of frequency, and $S(f)$ is the displacement spectrum of radiation at the source. In a homogeneous medium, $G(r, f)$ is equal to $1/r$ for body waves. At high frequencies, a widely accepted source spectrum model is the ω^{-2} model, which assumes that $S(f)$ is proportional to f^{-2} (Brune, 1970; Hanks, 1979). This model has been assumed to be valid in studying the attenuation of high-frequency waves from teleseismic sources (Der and McElfresh, 1976, 1977; Lundquist and Cormier, 1980; Der *et al.*, 1982; Der *et al.*, 1985), and for regional distance (local earthquakes) (Modiano and Hatzfeld, 1982; Hough and Anderson, 1988; Hough *et al.*, 1988). Since our primary interest is not the absolute value of t^* but its spatial variation within the crust, assuming a ω^{-2} model should cause no difficulties in our conclusion. Under this

assumption, $A_Q(r, f)$ in (1) becomes independent of frequency. In other words, equation (1) can be rewritten, after taking the natural logarithm on both sides, as

$$\ln A(r, f) = \ln A_Q(r) e^{-\pi f t^*} \tag{4}$$

The term $A_Q(r)$, in equation (4) includes the geometric spreading effect which is generally independent of frequency. Since the spreading effect is frequency-independent, the value of $A_Q(r)$ only affects the level of the spectrum but has no effect on the observed t^*. If Q is frequency-independent, then t^* is also frequency-independent. Thus, equation (4) can be differentiated with respect to f to obtain the relationship in Equation (5),

$$\frac{d(\ln A(r, f))}{df} = \pi t^* \tag{5}$$

which defines the slope of the straight line described by equation (4). The value for the slope, $-\pi t^*$, is determined by fitting the observed spectrum with a straight line by using a least-square method over a frequency range extending somewhat beyond the corner frequencies. For the earthquakes used in this study, the corner frequencies range from about 1 to 4 Hz. The lower and upper values (4 and 25 Hz are chosen in this study) are limited by the corner frequency and the uncertainty in instrument correction above 40 Hz, respectively.

However, many indications have pointed out that Q is frequency-dependent in the crust under the continental regions, at least at frequencies near 1 Hz (for example: Mitchell, 1980), and the degree of the dependence varies regionally (Mitchell, 1981). But unfortunately, it is almost impossible to investigate the frequency-dependency of Q with the data available in this study. Since our primary goal is to find the spatial variations of attenuation in the upper crust of the Taiwan area, the use of frequency-independent attenuation is justified.

3. DATA AND COMPUTATION

The Taiwan Telemetered Seismographic Network (TTSN) has monitored the seismicity in the Taiwan area since 1973 and was converted to digital recording in 1987. Digital seismograms from 98 local events in the network region were used to obtain the body-wave spectra. The magnitudes of these earthquakes range from 2.2 to 5.7. Figure 2 shows the location of these earthquakes and the seismic stations used in this study. The first 2.0 s starting from the onset times of the seismograms were analyzed for P phase. In order to examine whether the length of the time window would affect the calculated t_P^* value, several different window intervals on seismograms were tested. Three of them, with lengths of 1, 2, and 3 sec, are shown in Figure 3a and the spectra with the fitting lines for determining t^* for these three cases are shown in Figure 3b, 3c, and 3d. The t^* values are 0.02255, 0.02243 and 0.2262 sec respectively. Obviously, these values do not show any significant difference. This implies that the choice of time duration for analysis need not be emphasized.

The FFT method was used for studying the P phase spectra. Because the spectrum for frequencies lower than the corner-frequency and eigen-frequency are rather unreliable, and that for those higher than 25 Hz has a very small amplitude due to a high cut-off filter in the recording system, a frequency range from the corner frequency to 25 Hz is chosen in this

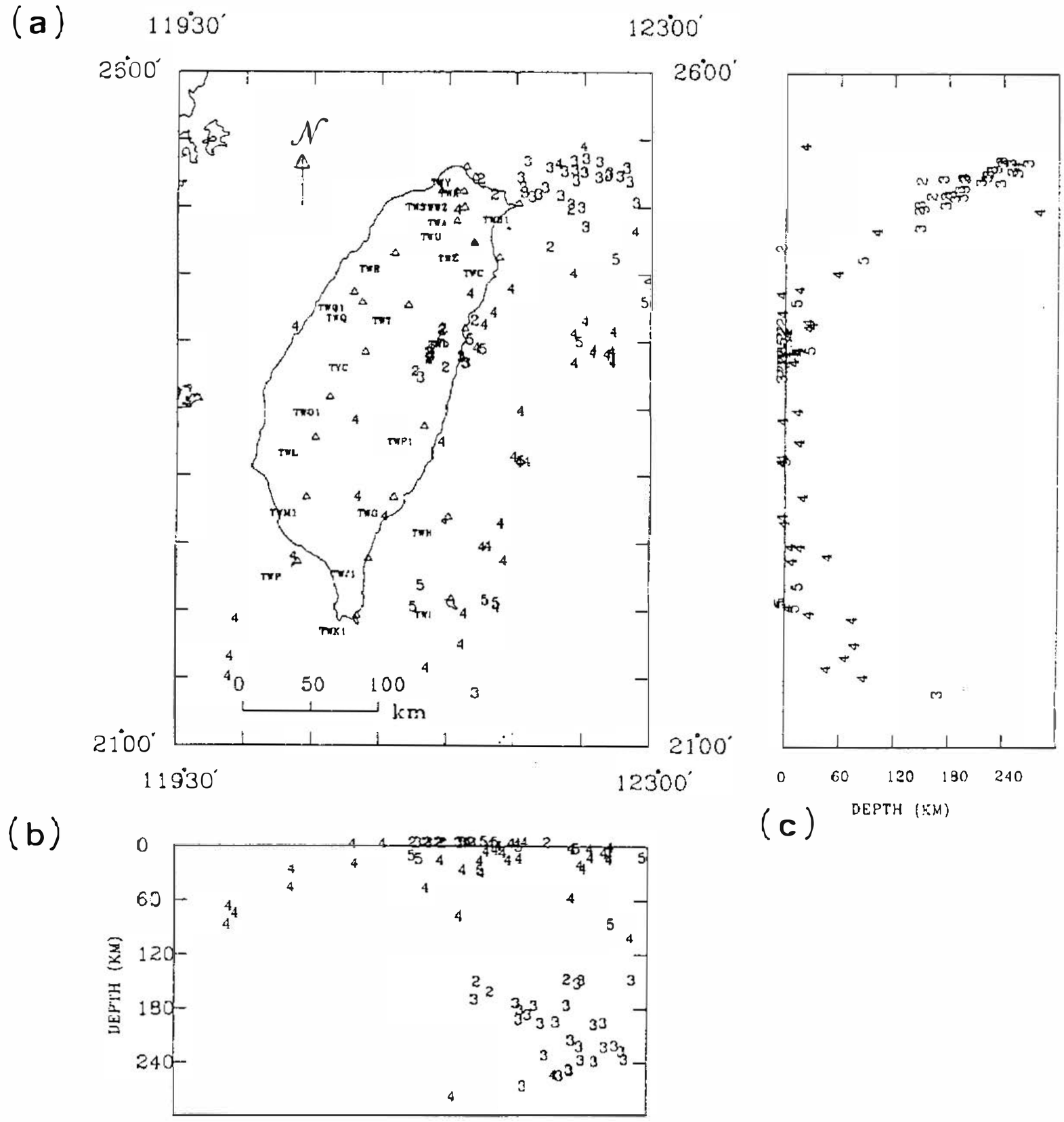

Fig. 2. Earthquakes and stations used in this study.

study. The slope for the power spectrum versus frequencies was determined by using the method of least squares. The procedure for determining the spectrum and calculating the attenuation of body waves is basically the same as that used by Hough *et al.* (1988) to calculate the attenuation of P and S waves and Al-Shukri *et al.* (1988) to calculate attenuation for the P wave only. The only difference between the present study and that of Hough *et al.* (1988) is that we use a Parzen window, whereas they used a cosine window before spectral analysis. It is found that the Parzen window produced a smoother spectrum than the cosine window did. Consequently, it enables us to eliminate the need for smoothing the spectrum before fitting the general trend with a least-squares method.

4. LINEARIZED INVERSION FOR P-WAVE ATTENUATION

A least-square inversion scheme was developed to determine a three-dimensional image of attenuation within a specific volume of the Earth beneath a local or regional seismic network. The data used for this technique are the observed t^* values calculated from P waves. The inversion procedure starts by dividing the volume of the Earth beneath the network into a number of layers, each layer being subdivided into a number of right rectangular prisms (blocks)

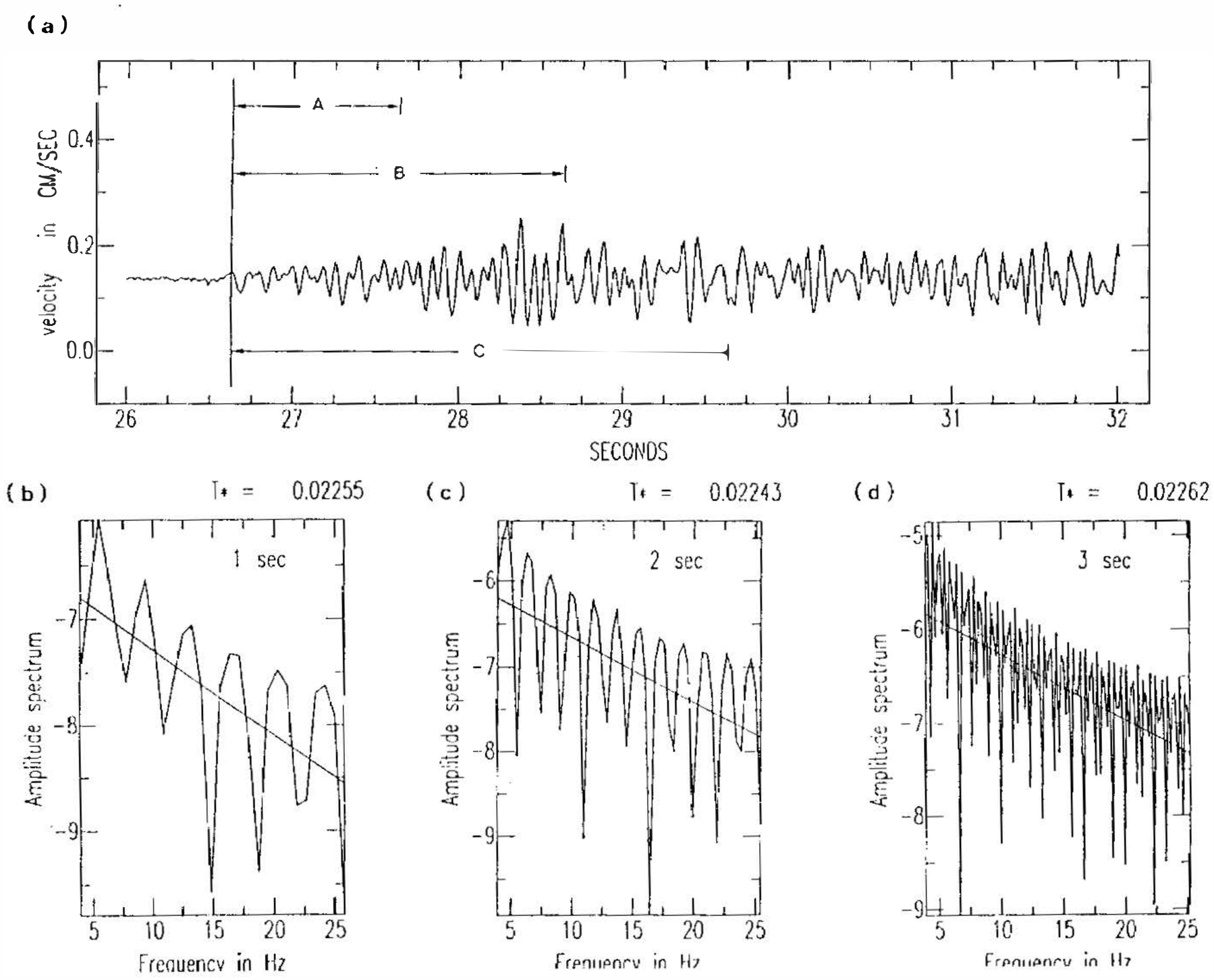

Fig. 3. (a) Seismogram used for calculating the t^* value and the three different time windows (denoted by A, B, and C);(b), (c) and (d) are the spectra calculated from the data truncated by time windows A, B, and C, respectively. The regression line and the t^* value are also shown in each diagram.

in which both the velocity and attenuation are assumed to be constant. We denote the attenuation within each block as Q_i^{-1} where i is an index to identify each block. The discretion permits the calculation of the initial t^* (t_o^*) for each ray that traverses the starting model. For a crustal model with discrete values of velocity and Q_i^{-1} in each block, equation (2) becomes

$$\delta t_o^* = \sum_{i=1}^{N} t_{io} Q_{io}^{-1} \delta_i \qquad (6)$$

where N is the number of blocks in the model, δ_i is a delta function equal to unity inside each block that has been traversed by a ray and zero elsewhere, Q_{io}^{-1} is a value for attenuation and t_{io} is a value for the travel time in blocks of the initial model. Assuming that the observed t^* (t_{ob}^*) can be parameterized in a function similar to that in equation(6), the difference between t_{ob}^* and t_o^* can be written as

$$\delta t^* = \sum_{i=1}^{N} t_{io} \left(\frac{t_{iob}}{t_{io}} Q_i^{-1} - Q_{io}^{-1} \right) \qquad (7)$$

where Q_i^{-1} is the unknown value of attenuation in each block. For M observations, a set of equations can then be formed as

$$\begin{bmatrix} \delta t_1^* \\ . \\ . \\ . \\ \delta t_N^* \end{bmatrix} = \begin{bmatrix} t_{11} & t_{21} & . & . & t_{m1} \\ t_{12} & . & . & . & . \\ . & . & . & . & . \\ . & . & . & . & . \\ t_{1N} & . & . & . & t_{MN} \end{bmatrix} \begin{bmatrix} \delta Q_1^{-1} \\ \delta Q_2^{-1} \\ . \\ . \\ \delta Q_M^{-1} \end{bmatrix} \tag{8}$$

where δQ_i^{-1} is the unknown attenuation perturbation $(Q_i^{-1} - Q_{io}^{-1})$ for the ith block through which rays have traveled for a particular period of time. Note that t_{ij} in (8) is the theoretical travel time in the ith block from the jth observation. Equation (8) can be rewritten in matrix form as

$$\mathrm{Y} = \mathbf{T}\,\boldsymbol{q} \tag{9}$$

where Y is the δt^* vector, $\mathbf{T}$ is the travel-time matrix, and $\boldsymbol{q}$ is the unknown vector of attenuation. A stochastic least-squares solution to (8) is given by

$$\hat{q} = [\mathrm{T}^{\mathrm{T}}\mathrm{T} + \theta^2 I]^{-1}\mathrm{T}^{\mathrm{T}}\mathrm{Y} \tag{10}$$

where $\hat{\boldsymbol{q}}$ is the approximate solution of $\boldsymbol{q}$, θ^2 is the damping parameter with a positive value, and $\mathbf{I}$ is the identity matrix. Equation (9) is set to be overdetermined due to the expected errors in computing t^*_{ob} using the spectral decay technique. The stochastic least-square solution is preferred because it is more stable than the undamped solution. The resolution matrix for the solution is given by

$$R = [\mathrm{T}^{\mathrm{T}}\mathrm{T} + \theta^2 I]^{-1}\mathrm{T}^{\mathrm{T}}\mathrm{T} \tag{11}$$

and the covariance matrix by

$$C = \sigma_{\mathrm{d}}^2[\mathrm{T}^{\mathrm{T}}\mathrm{T} + \theta^2 I]^{-1}\mathrm{T}^{\mathrm{T}}\mathrm{R} \tag{12}$$

where σ_{d}^2 is the variance of error in the data. The standard errors of the solution equal to the square roots of the diagonal elements of $\mathbf{C}$. The above scheme permits us to obtain the final solution interactively and to examine the convergence of the solution at each step.

The essential step of the forward solution for setting up equation (8) is the calculation of the travel-time matrix. The travel-time traced by a ray in each individual block was calculated by using a ray tracing algorithm in which blocks are assumed to be homogeneous and rays within these blocks are approximately characterized by straight-line paths. Thurber and Ellsworth (1980), using numerical integration through a heterogeneous medium, have shown an excellent approximation to the actual travel time. In this study, a numerical integration procedure similar to the one used by Thurber and Ellsworth (1980) was employed to calculate the travel time. First, the ray is divided into a number of segments having equal lengths. Then, the travel time for each segment is calculated and the times of all segments belonging to the same block are added together to form the total travel time in that block. If a ray hits a block or a layer boundary, the length of the segment is modified to be the distance between the end of

the last segment and the boundary. The travel time for this modified segment was calculated accordingly.

The inversion procedure was tested extensively. Both homogeneous and heterogeneous models were first used to generate synthetic data for t^*. These data were then inverted by using a number of different starting models. In the foregoing calculations, the initial value of Q_p was set to 0. Then the average Q_p value was estimated and used to check the dependence of results for initial values. An average Q_p of 0.0005 was obtained. The results indicated that the initial values do not influence the evaluated Q_p values to any great extent. In all cases, with sufficient numbers of observations, solutions using error-free synthetic data converged perfectly with the expected solutions. The errors of the final solution are usually less than the level of the data errors.

5. RESULTS AND DISCUSSIONS

In this study, a number of combinations of initial velocity and Q_p models have been used to invert the 1620 t^* observations. One of them is presented here. The distribution of the Q_p values obtained in each block is shown in Figure 4. Generally speaking, the standard errors in Q_p are less than 10 (for an example, see Figure 4). To easily investigate the characteristics of the Q_p structures, contour lines for different layers were also made and presented in Figure 5.

For the top layer (depths of between 0 and 5 km), the Q_p values range from 11 to 943 (Figure 4b). About 63% of the Q_p values are less than 200. Two Q_p highs were found: one at the northern part of the Central Range, and the other at the Southern tip of Taiwan island. The lateral variances of attenuation in the top layer indicate that the alluvial layer, which covers the southwest part of the region, might have little effect on the Q_p values. It is known that the thickness of alluvium increases gradually to the Southwest and reaches a maximum thickness of about 1 km in the extreme southwestern portion of the region studied. However, if the alluvium had a measurable effect on Q_p, a trend of increasing Q_p values should be parallel to the increase in thickness. In fact, Figure 4b shows no such trend. In addition, the model shows no difference in attenuation between the northern part of the region and the southwestern part where the alluvium is about 1 km thick, indicating that the alluvial cover has only a very small effect on the Q_p values in the blocks.

In layer 2 (depths of between 5 and 10 km), the Q_p values range between 20 and 943 (Figure 4c). About 53% of the Q_p values are less than 200. The average for this layer is 220. The lowest value occurs in a region of intense earthquake activity, while the highest values occur in the outer blocks far away from the active region.

In the depth range of 10 to 15 km (layer 3), the Q_p values range from 35 to 833 (Figure 4d). The average for this layer is 265. About 55% of Q_p values are less than 200. The standard error of each block is slightly less than 1.

In the depth range of 15 to 25 km (layer 4), the Q_p values are distributed from 31 to 827 (Figure 4e). Approximately 24% of the blocks have Q_p values less than 200. About 55% of the blocks have a Q_p value between 400 and 600. The average of this layer is 384. The average standard error for this layer is 2.

In the depth range of 25 to 35 km (layer 5), the Q_p values range between 49 and 1053 (Figure 4f). The variation is much smoother than for all its upper layers. The average of this

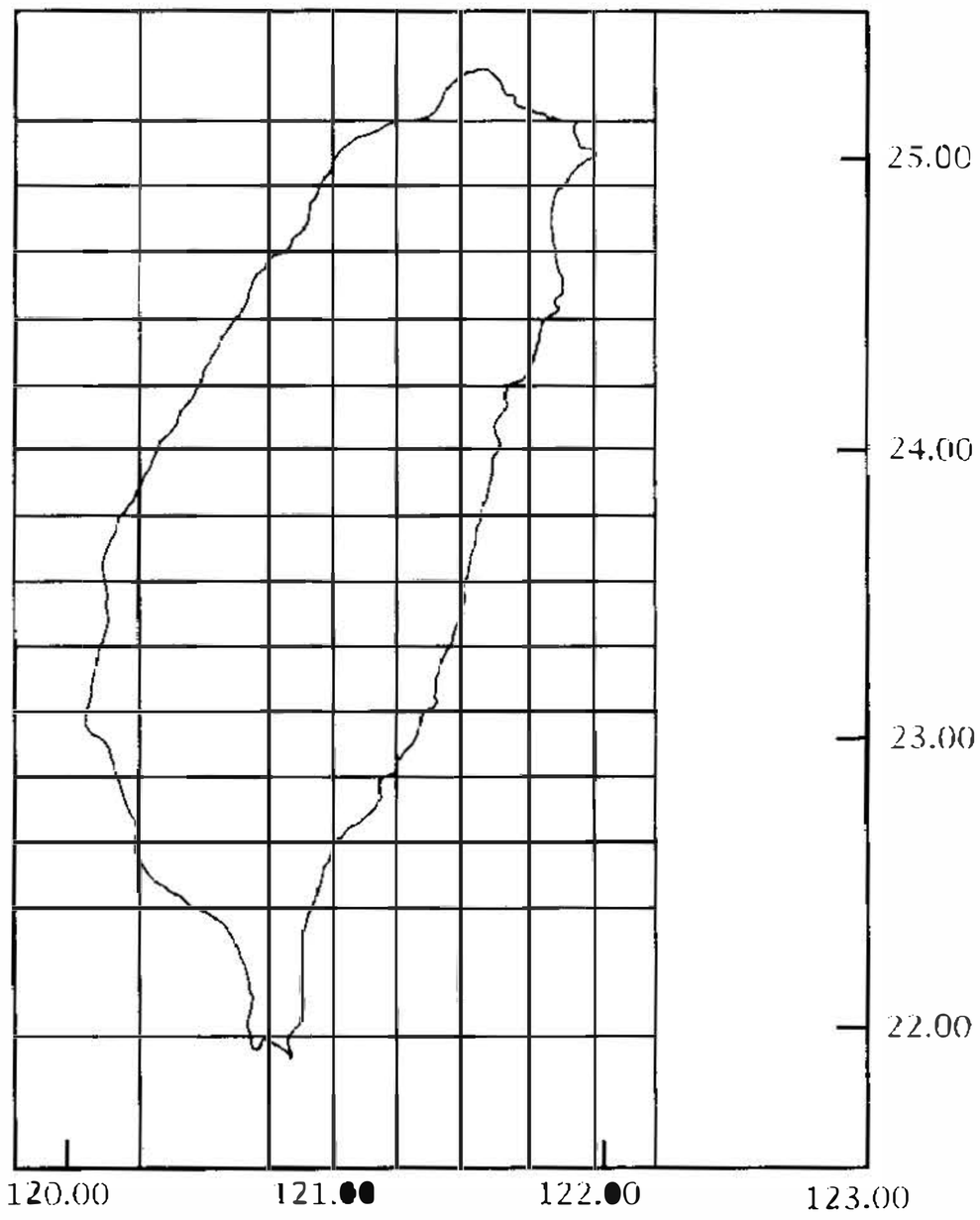

(a)

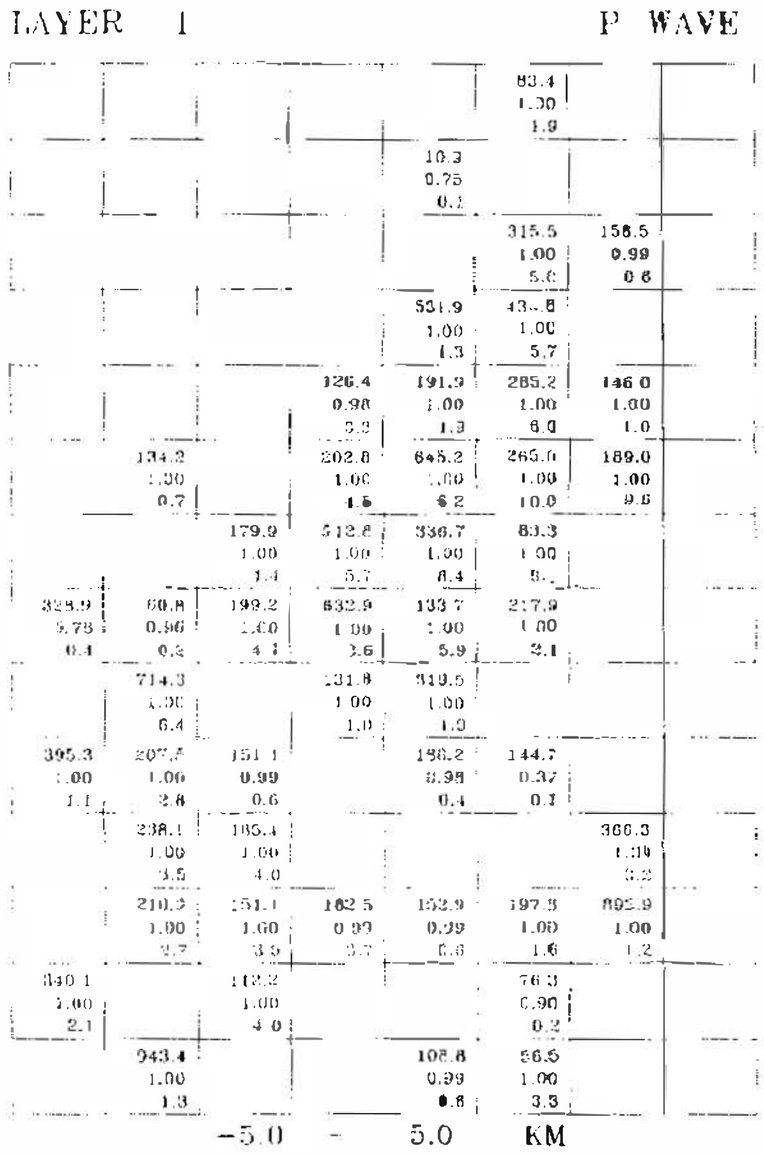

(b)

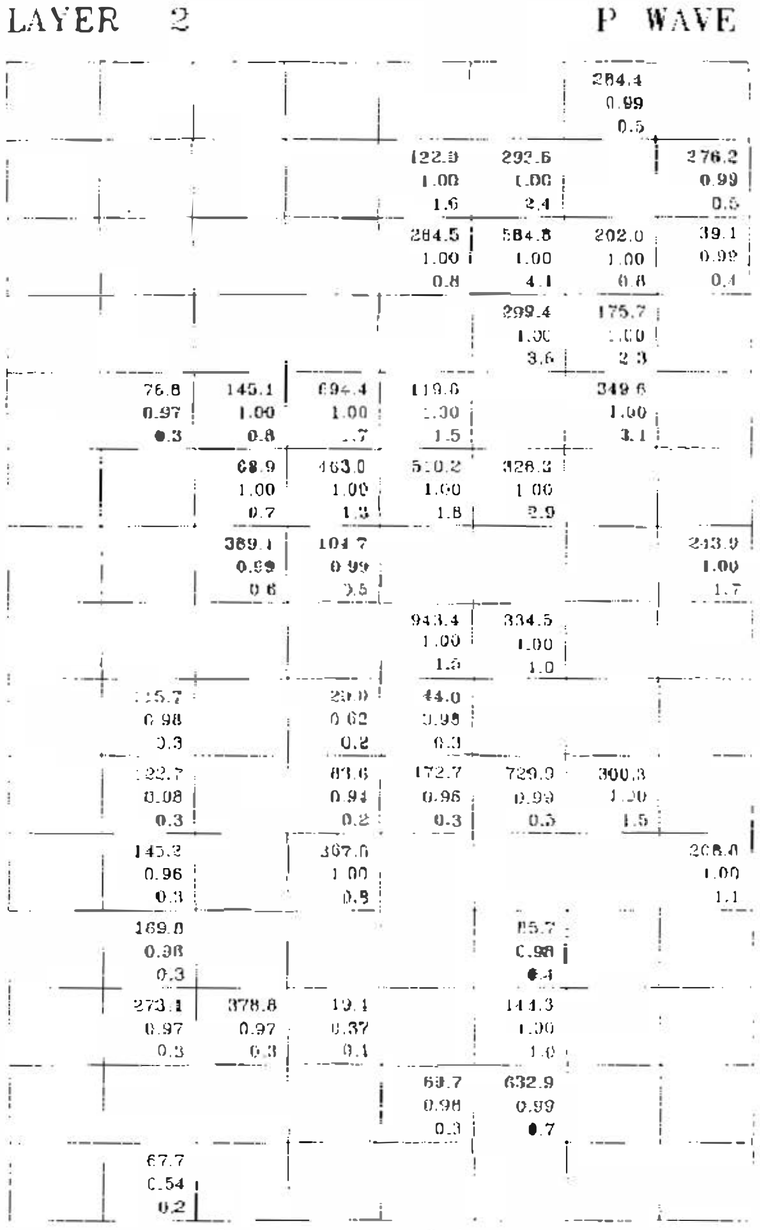

(c)

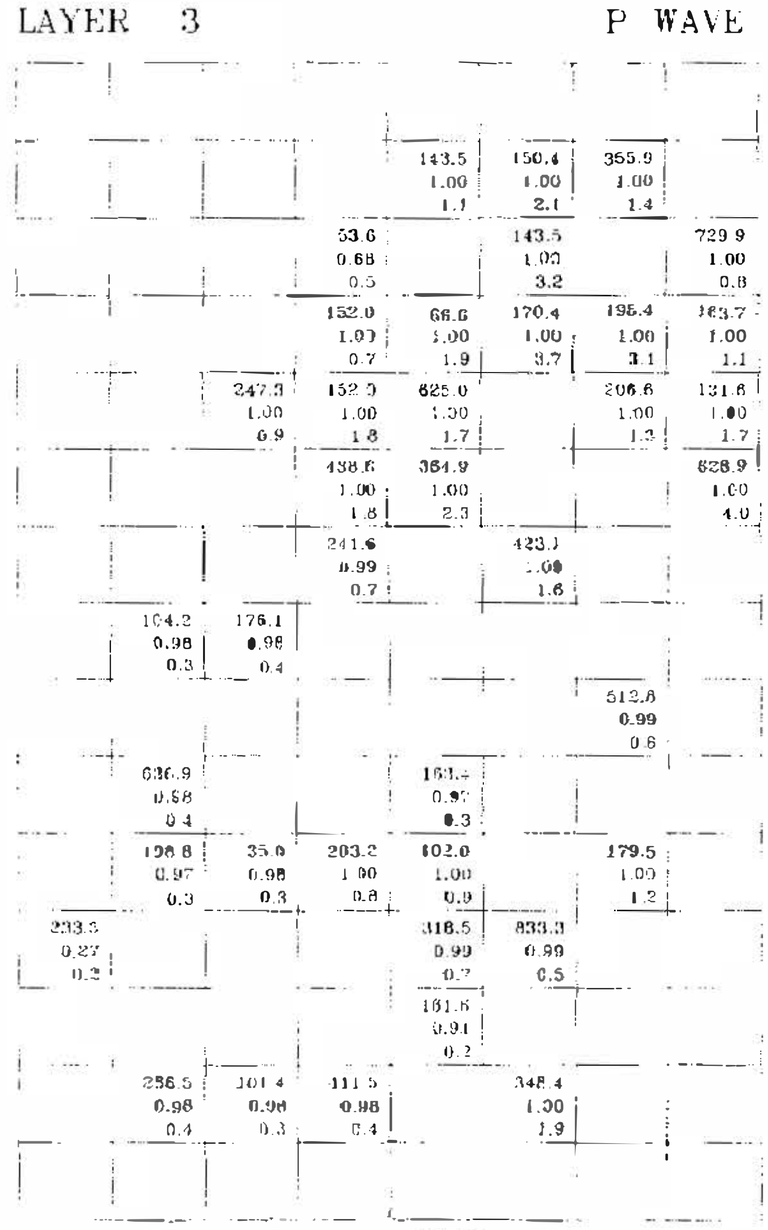

(d)

Fig. 4. (a) Positions of the blocks. (b)~(j) Results of the inversion for layers 1~9. The numbers in each box are the Q_p values, the diagonal of the resolution matrix, and the standard error determined from the diagonal covariance matrix and the standard deviation in t^*.

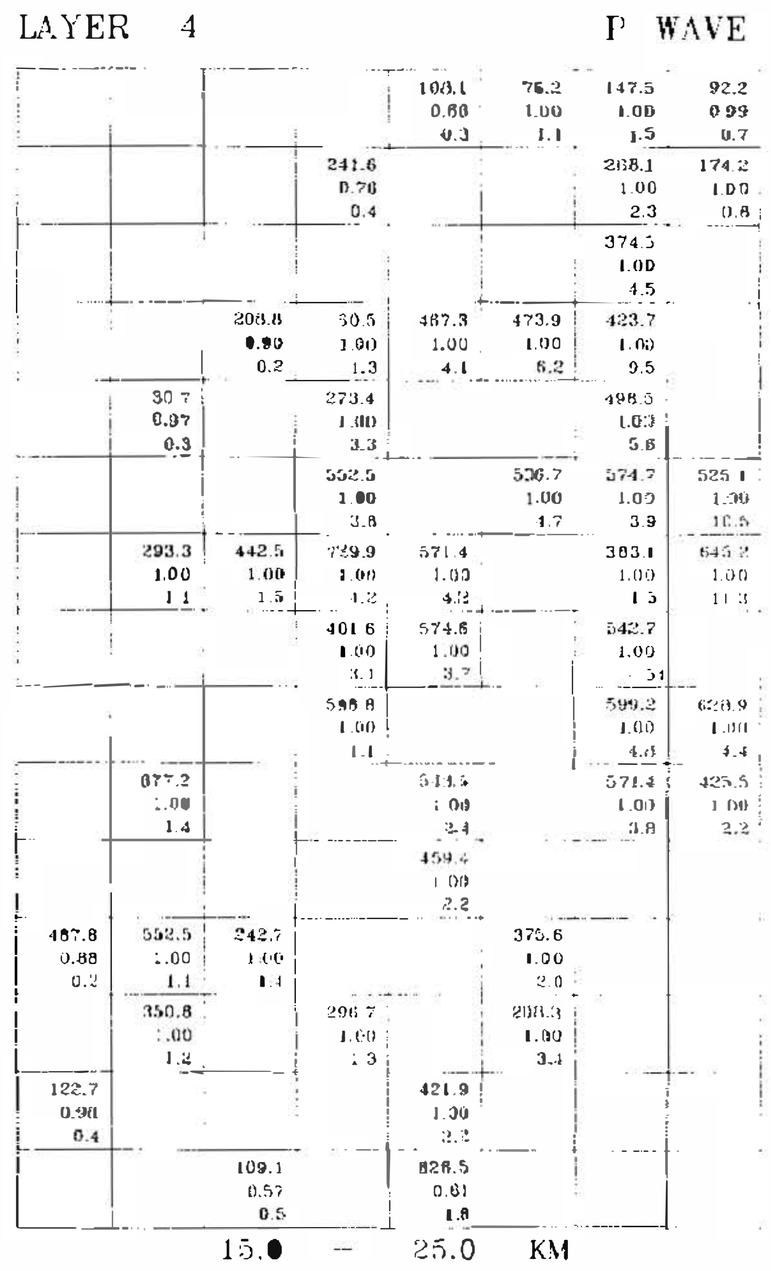

(e)

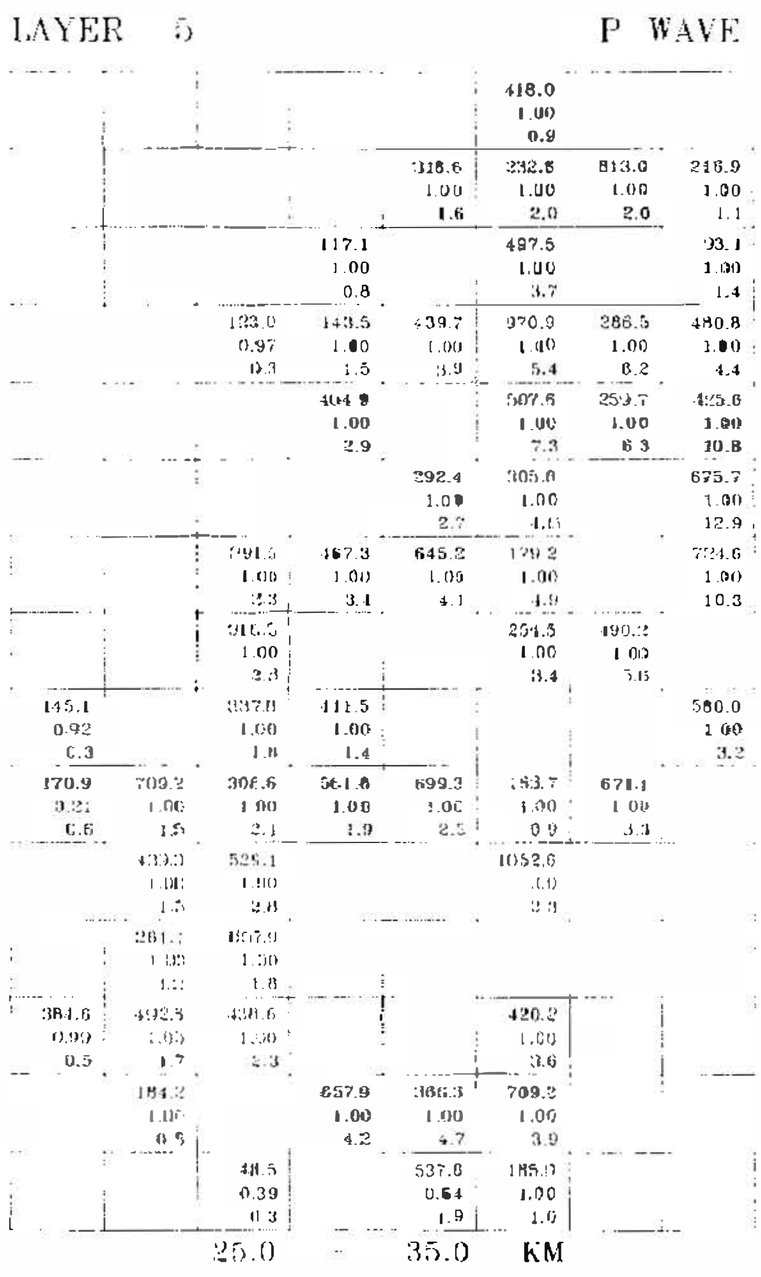

(f)

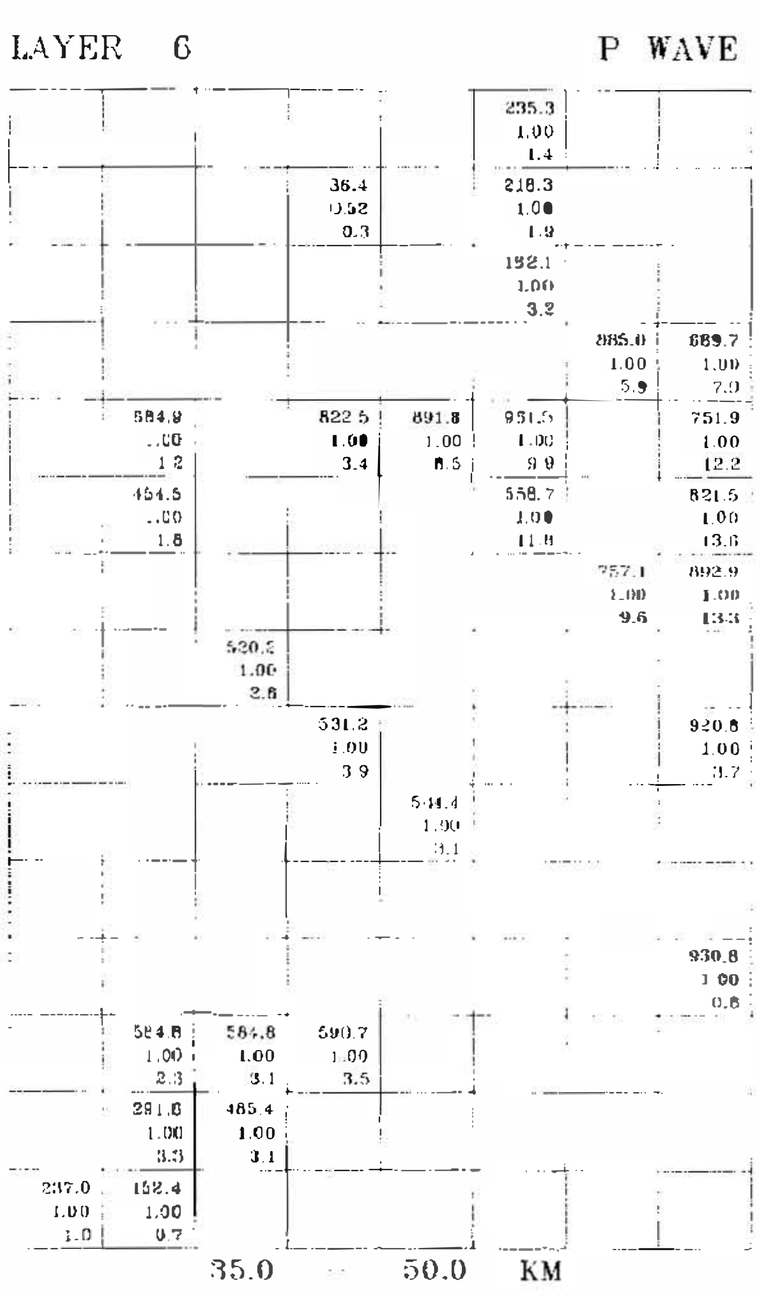

(g)

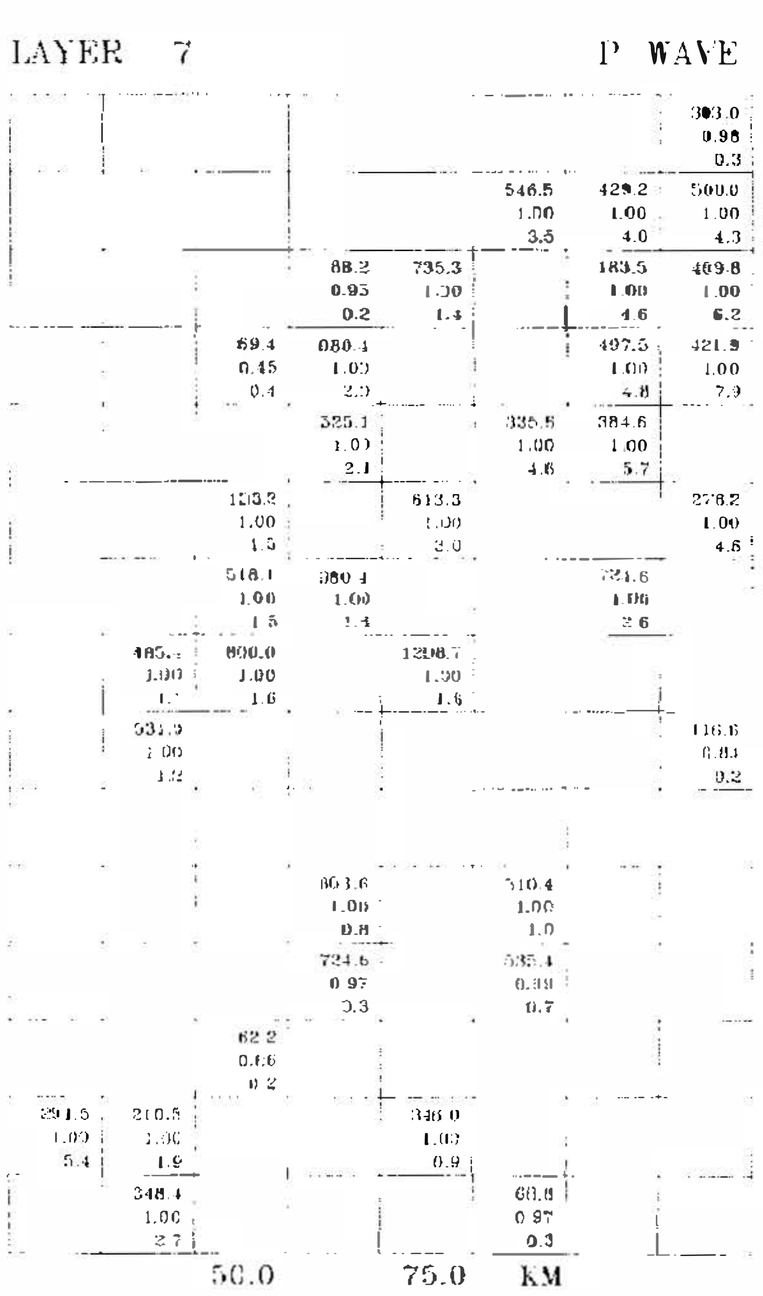

(h)

Fig. 4. (Continued.)

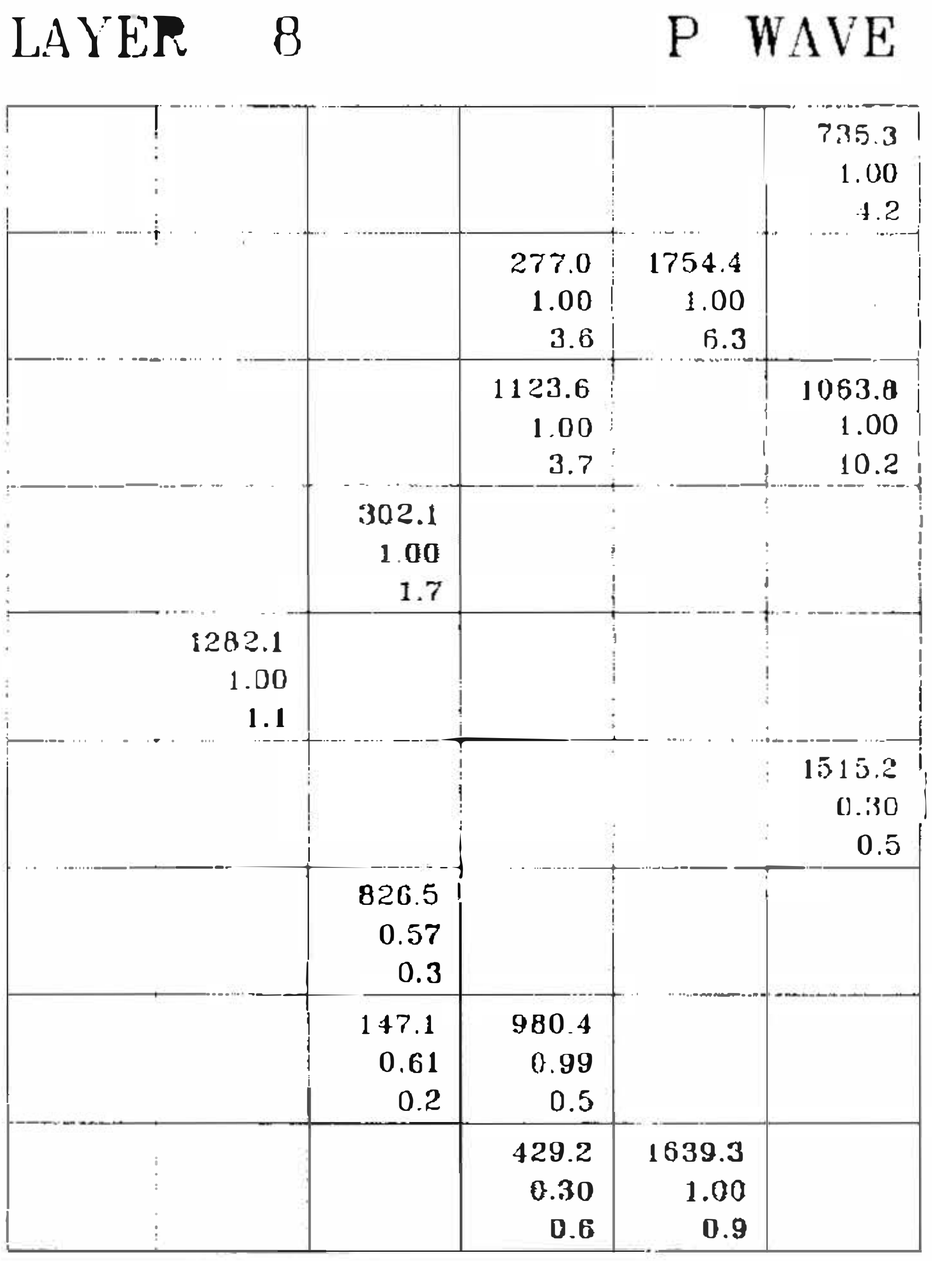

(i)

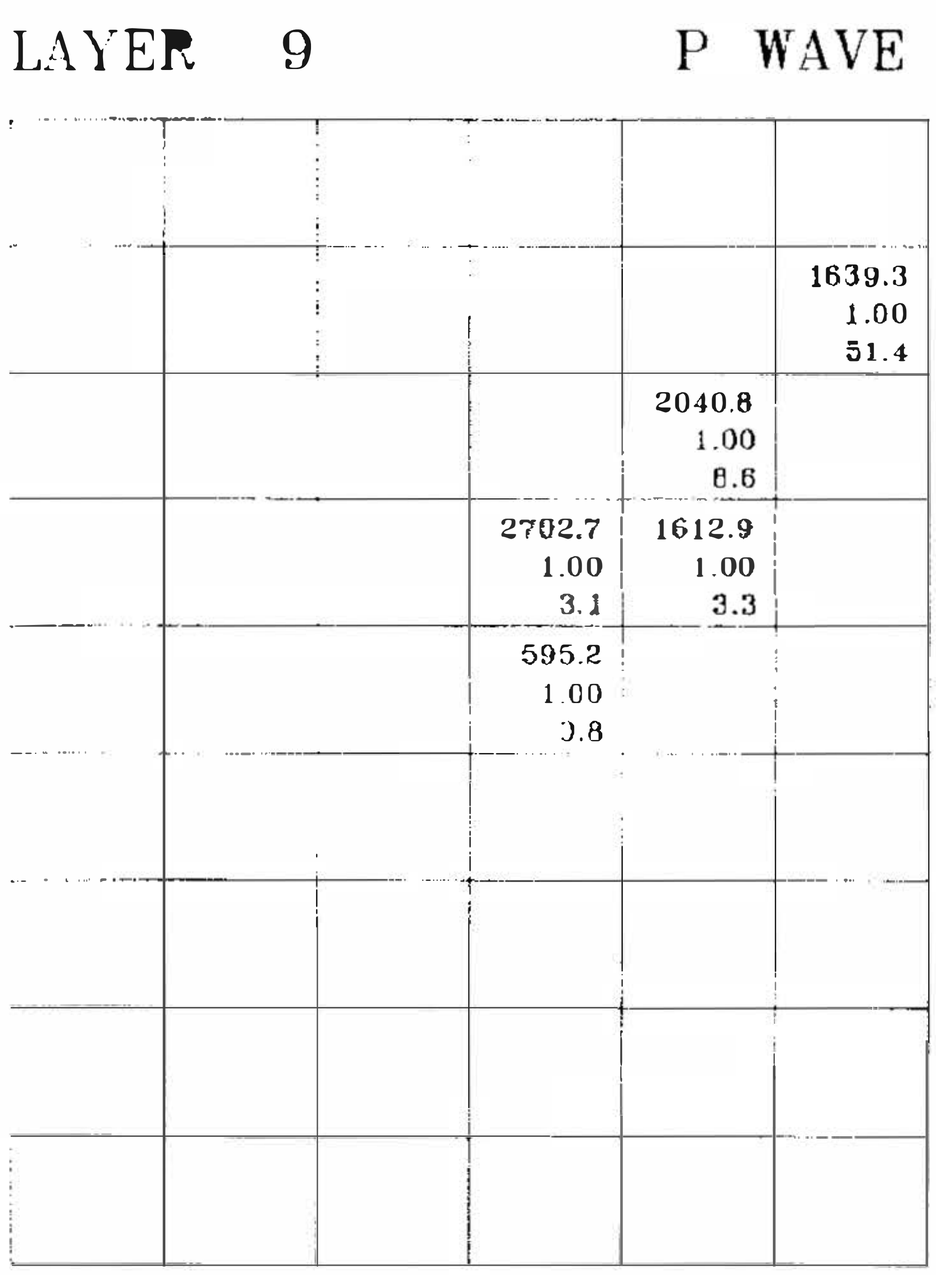

(j)

Fig. 4. (Continued.)

layer is about 404. About 50% of the blocks have *Qp* values less than 400. The standard error is slightly less than 2.

In the depth range of 35 to 50 km (layer 6), most of the Q_p values are greater than for its upper layers. They range between 36 and 962 (Figure 4g). The variation is much smoother than for all its upper layers. The average of this layer is about 586. About 43% of blocks have Q_p values less than 600. Only 10 % of the blocks have values less than 200. The standard error is slightly less than 3.

In the depth range of 50 to 75 km (layer 7), the Q_p values range between 62 and 1297 (Figure 4h). The Q_p values on the land are slightly greater than 400. The average of this layer is about 550. About 60% of the blocks have Q_p values less than 400. The standard error is slightly less than 2.

In the depth range of 75 to 100 km (layer 8), the variation of Q_p values is smoother than for all of its upper layers. The distribution pattern of Q_p values in this layer can be classified into three parts. The region in the southeast part, has a higher Q_p value, ranging between 800 and 1200 (Figure 4i). The Q_p values on the island are in the range of 500 to 700. The third part, to the west of the island, has a mean value of 900.

Lateral changes in Q_p values in the half space were not considered because only a few regions of the half space were passed by rays. Because of the limited coverage, we considered the half space to be homogeneous, and the value of Q_p given in the model represents an average value for depths a few kilometers below the lowest layer.

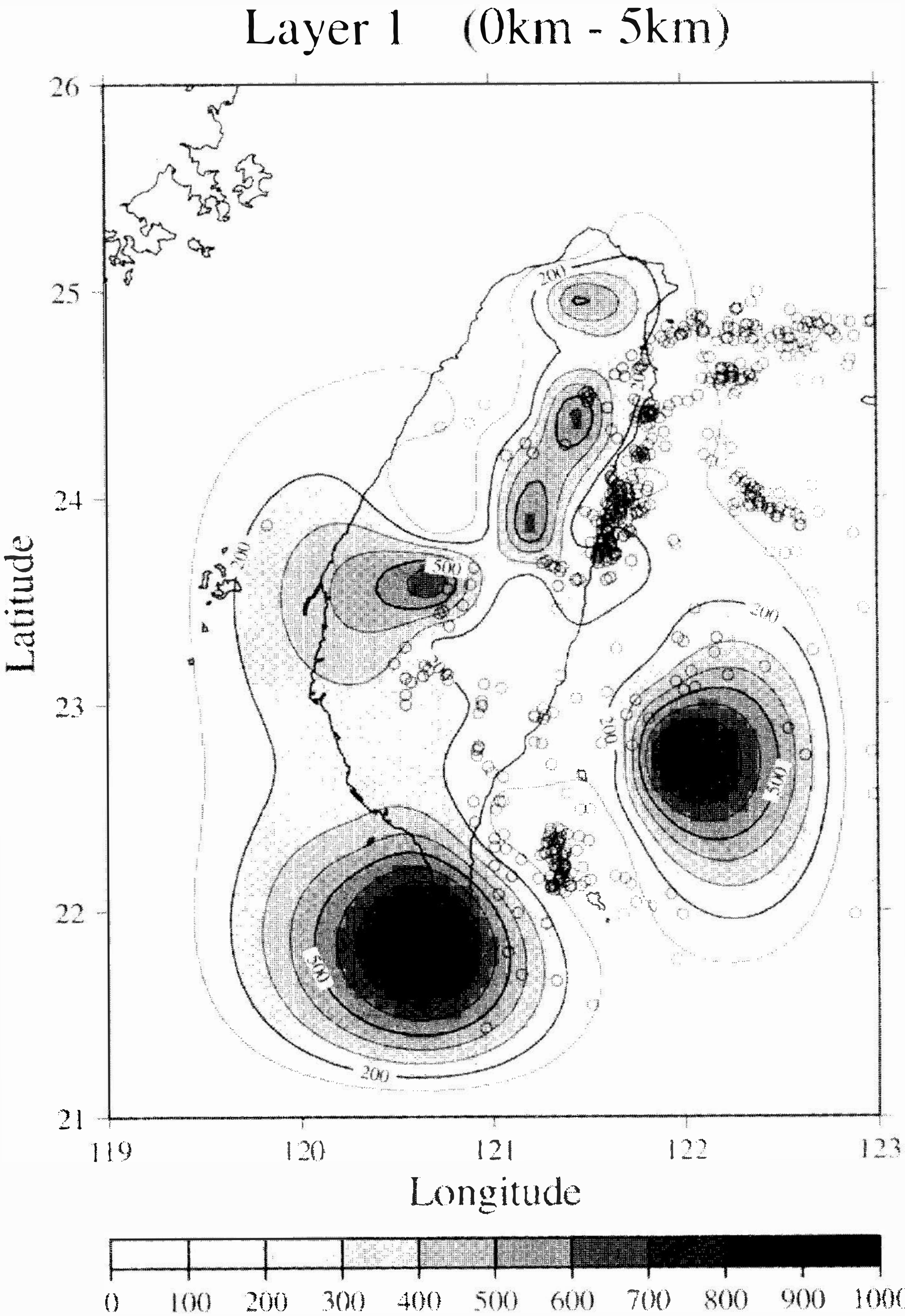

(a)

Fig. 5. Distribution of the Q_p values for each layer. These values are attributed to the center of each block, so that contour lines can be drawn. Contour lines are not drawn on zones through which no rays pass. Earthquakes located in the same block are shown with hollow circle symbols. The parameters of these earthquakes are mentioned in text.

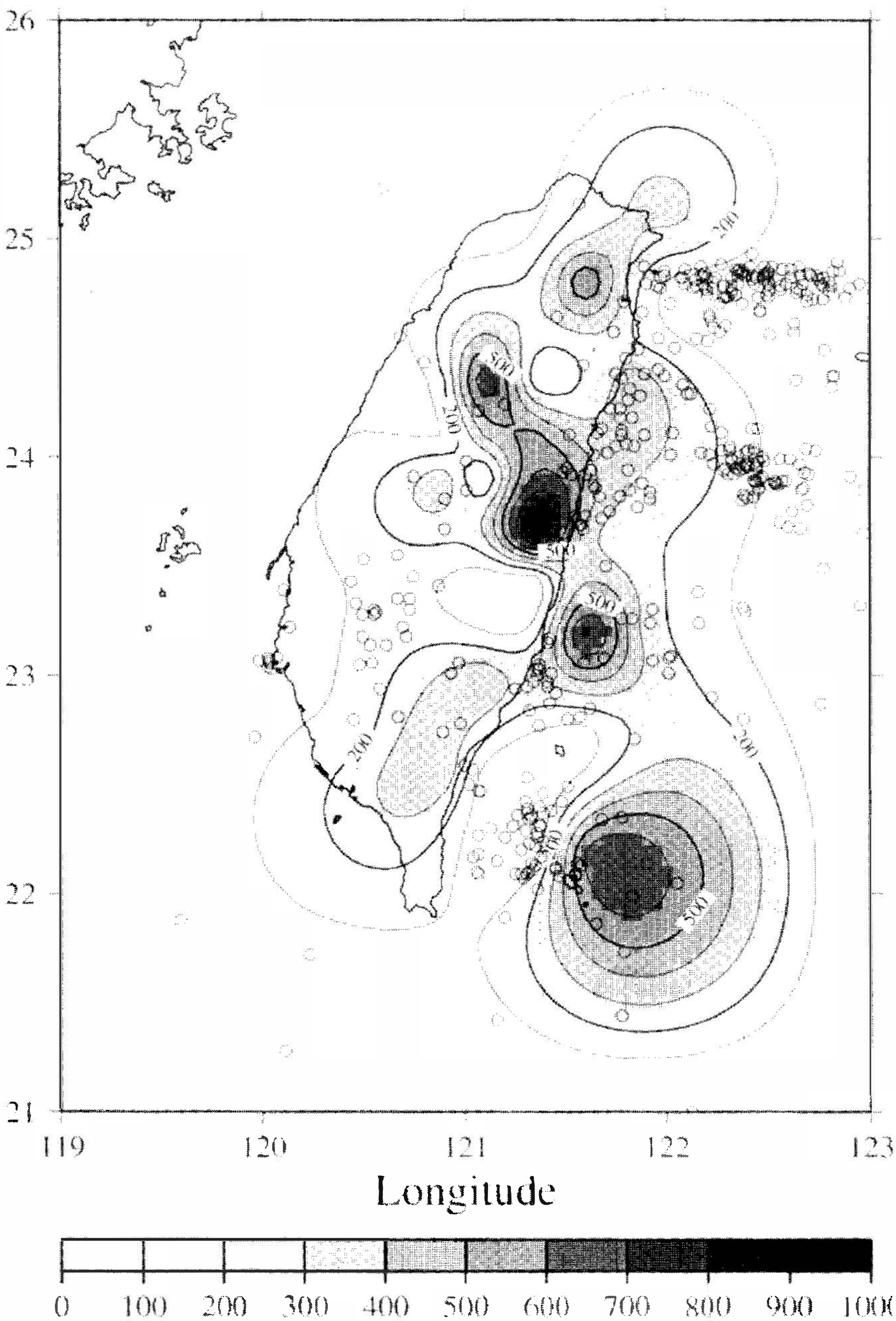

(b)

Fig. 5. (Continued.)

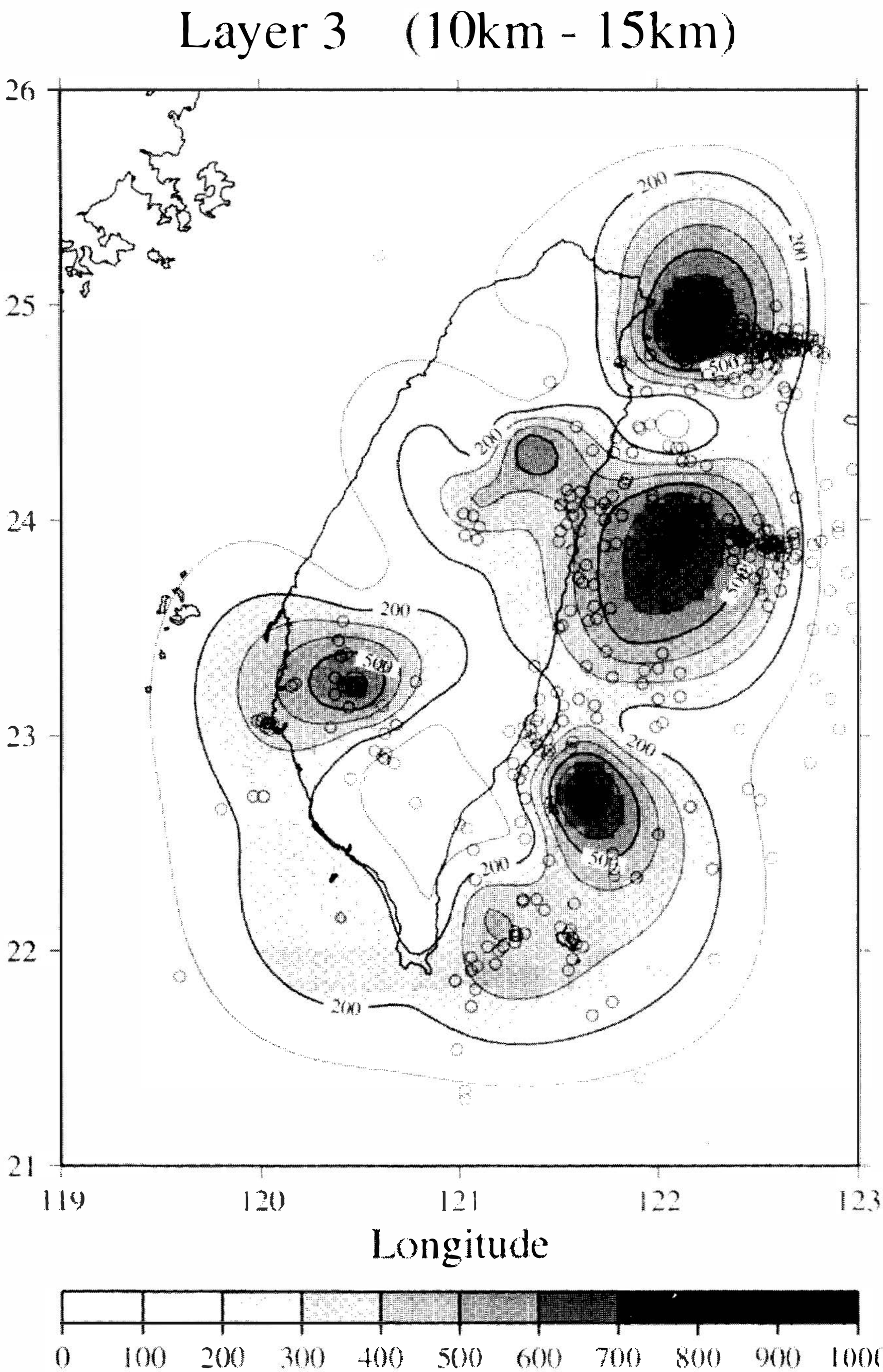

(c)

Fig. 5. (Continued.)

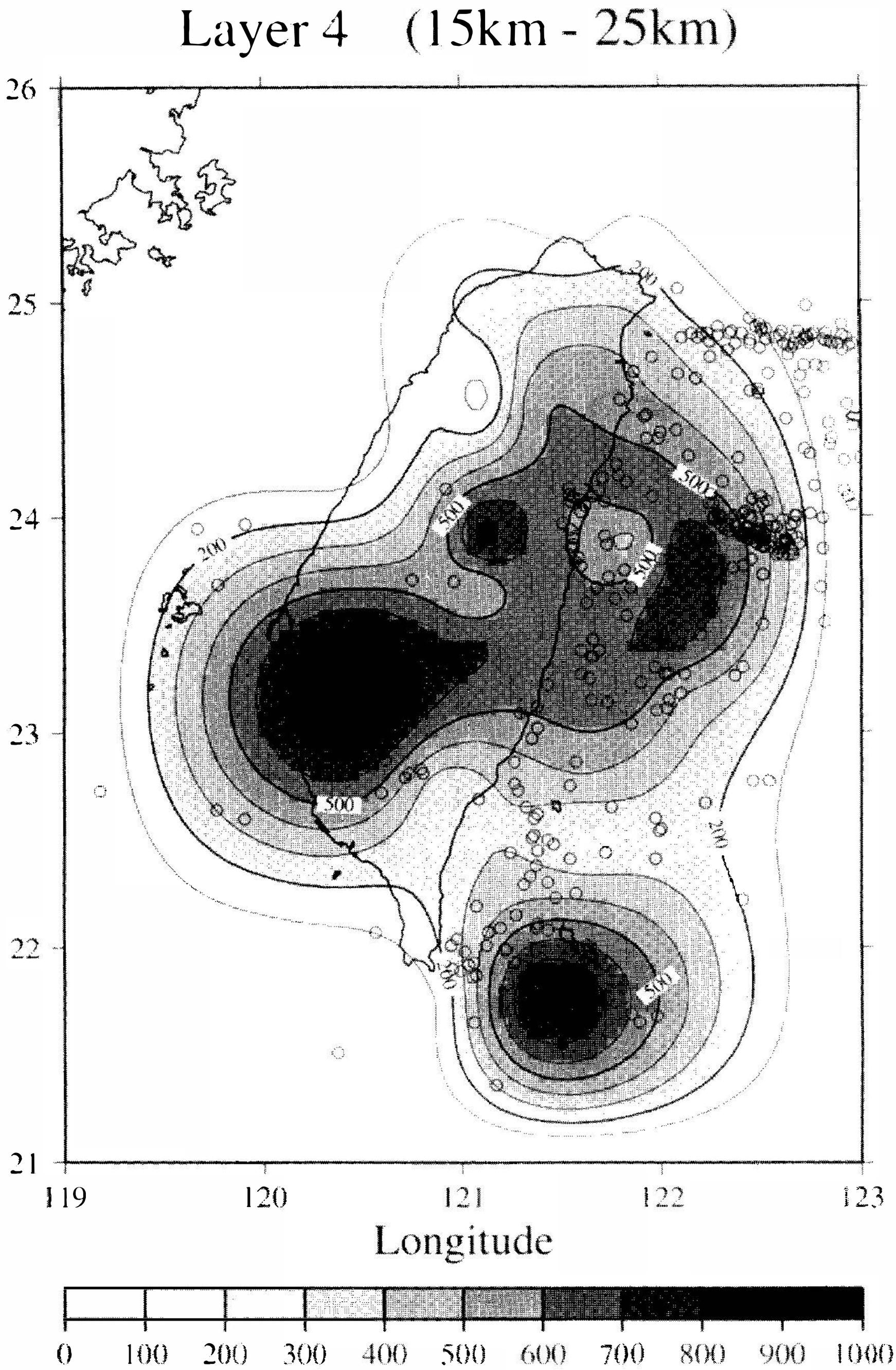

(d)

Fig. 5. (Continued.)

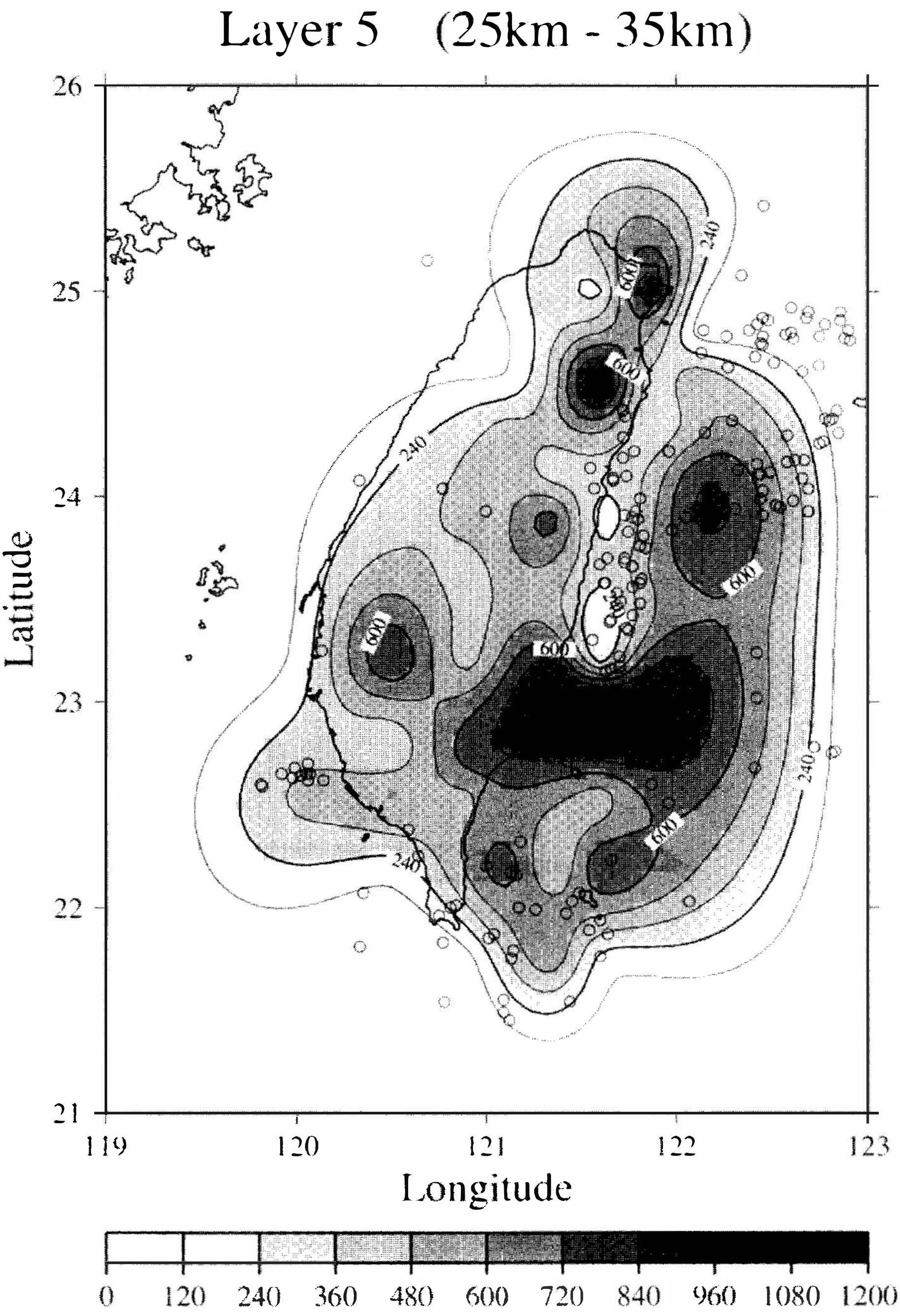

(e)

Fig. 5. (Continued.)

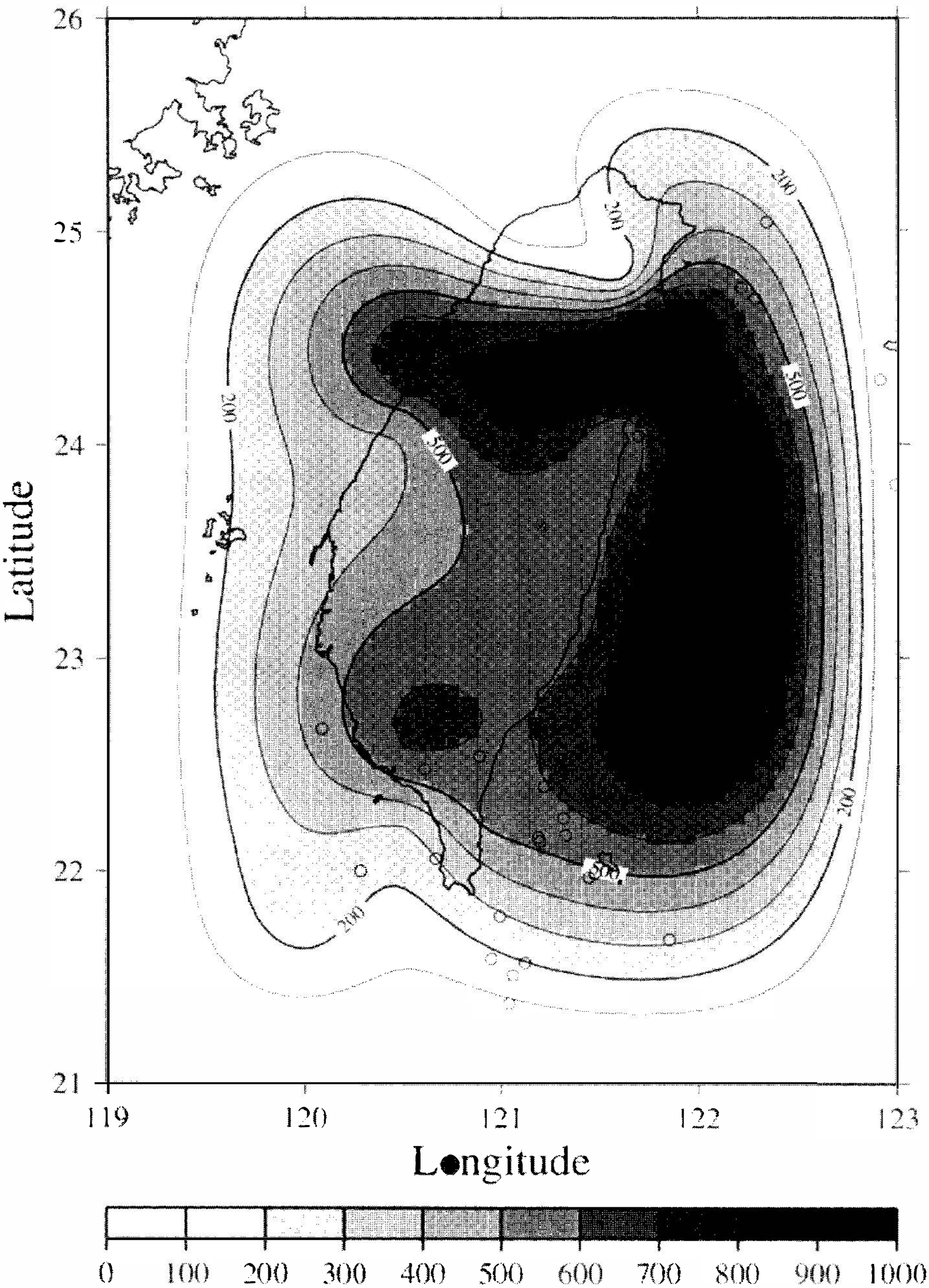

(f)

Fig. 5. (Continued.)

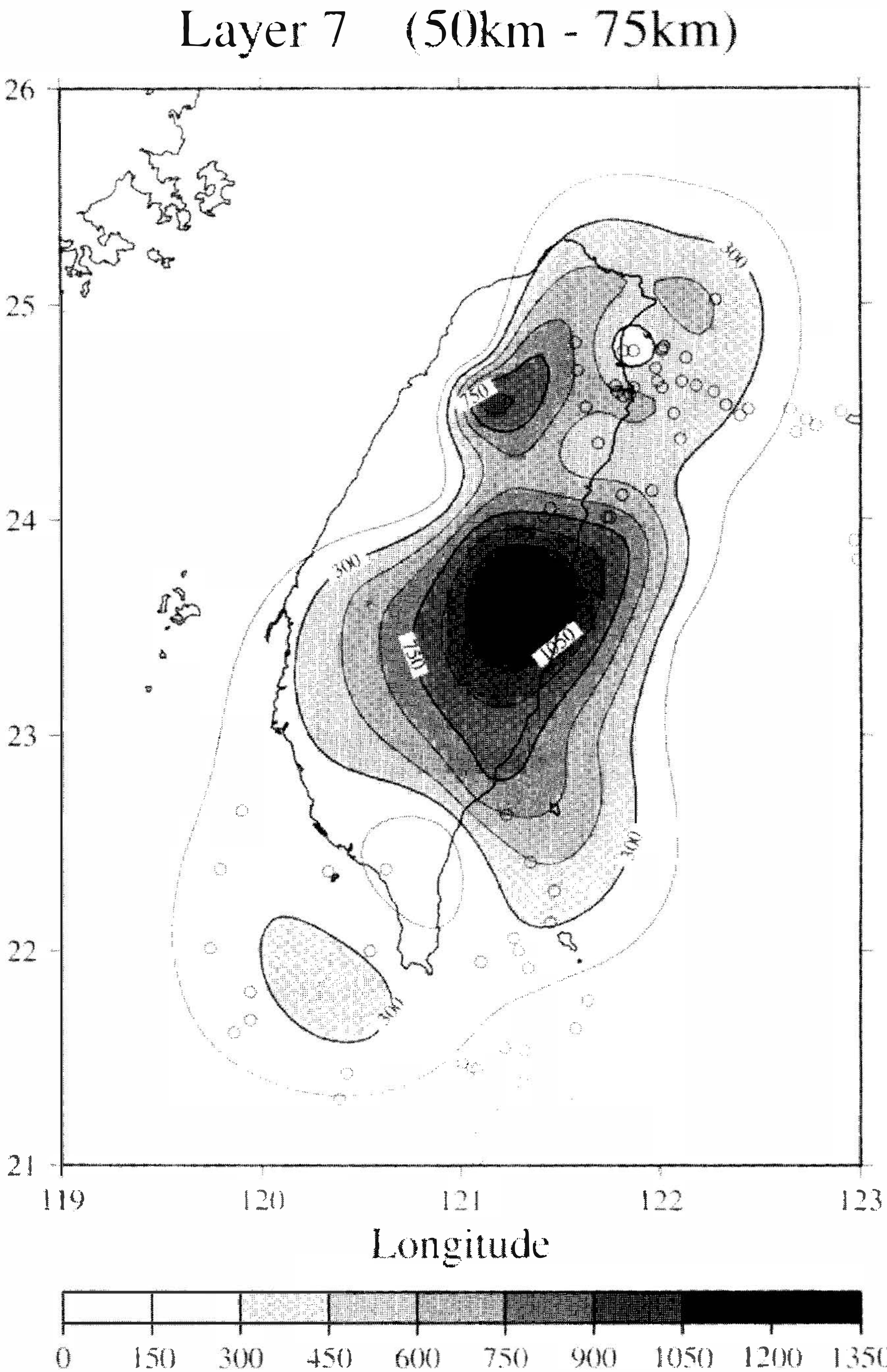

(g)

Fig. 5. (Continued.)

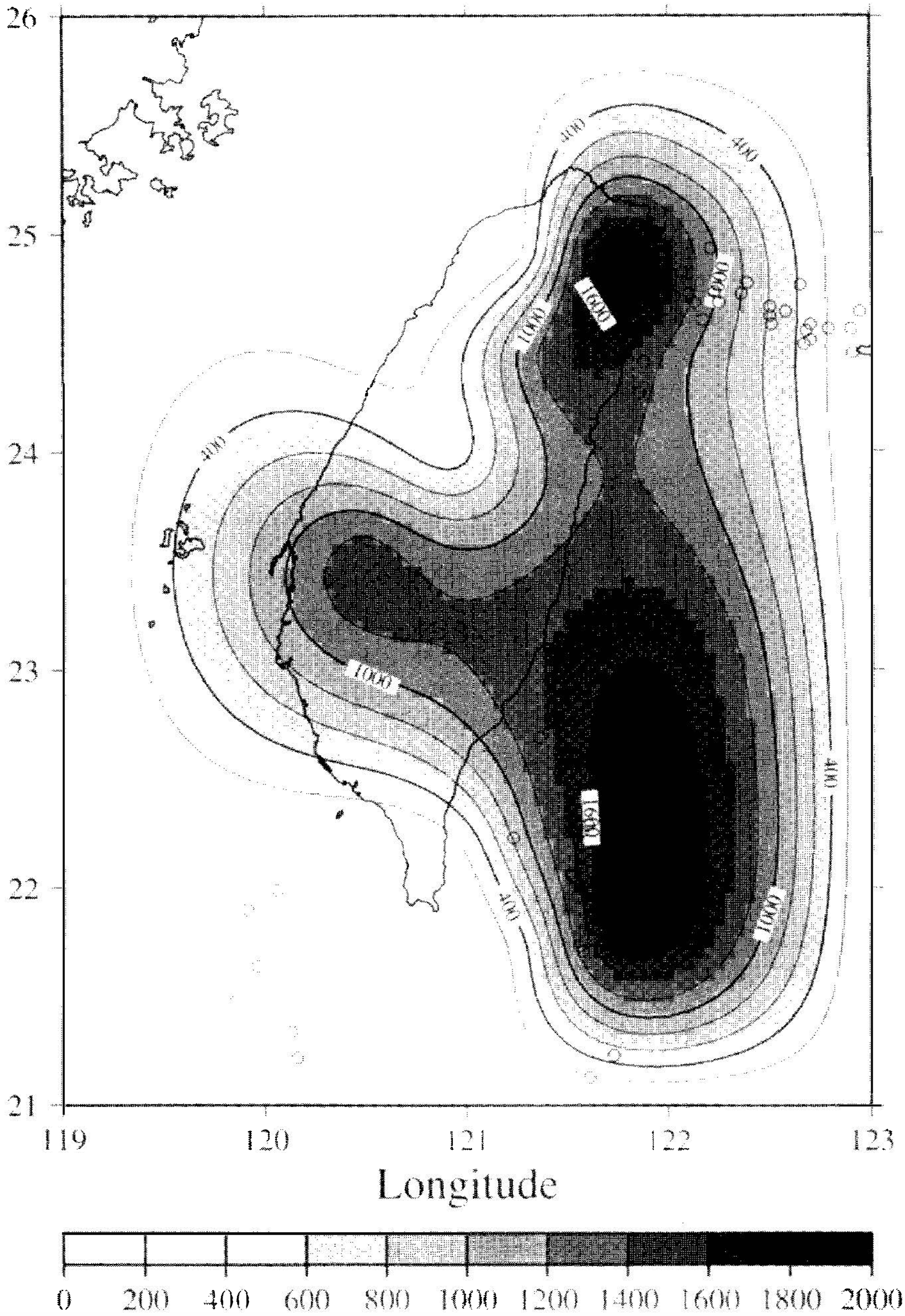

(h)

Fig. 5. (Continued.)

The earthquakes located in the region correlated to each layer are also plotted in the same panel of the Q_p structure (Figure 5). The magnitudes of these events are greater than 4.0. The distribution pattern correlates with a general increase of earthquake activity in the region. The lowest value of Q_p (62.5) occurs in the block that has the highest level of seismic activity. There is a slight increase in the Q_p value to the east of the high activity zone. This increase in attenuation correlates with a slight increase in seismicity. However, this block is a peripheral block and its value is not well-determined.

6. CONCLUSIONS

The results of the present study indicate that Q_p values in the Taiwan area are well-correlated to with seismicity. In the upper crust (at depths between 0 to 10 km), a lower Q_p area is consistent with a higher seismicity area. However, in the lower crust (10 to 25 km) and upper mantle, the higher seismicity area is consistent with higher Q_p value.

Acknowledgments The authors are grateful to their colleagues Messrs. Shen-Yen Lee and Cheng-Horn Yeh for assistance in data processing. We thank the TTSN group of our institute for providing part of the earthquake data. Thanks are also due to Dr. Ling-Yun Chiao for his valuable suggestions.

REFERENCES

Al-Shukri, H. J., B. J. Mitchell, and H. A. A. Ghalib, 1988: Attenuation of seismic waves in the New Madrid seismic zone. *Seism. Res. Lett.*, **59**, 133-139.

Brune, J. N. 1970: Tectonic stress and the spectra of seismic shear waves from earthquakes. *J. Geophys. Res.*, **75**, 4997-5009.

Der, Z. A., and T. W. McElfresh, 1976: Short period P wave attenuation along various paths in North America as determined from P wave spectra of the Salmon Nuclear Explosion. *Bull. Seism. Soc. Am.*, **66**, 1609-1622.

Der, Z. A., and T. W. McElfresh, 1977: The relationship between anelastic attenuation and regional amplitude anomalies of short-period P -waves in North America. *Bull. Seism. Soc. Am.*, **67**, 1303-1317.

Der, Z. A., T. W. McElfresh, and A. O'Donnell, 1982: An investigation of the regional variation and frequency dependence of anelastic attenuation in the mantle under the United States in the 0.5-4 Hz band. *Geophys. J. R. Astr. Soc.*, **69**, 67-100.

Der, Z. A. ,T.W. McElfresh, R. Wagner, and J. Burnetti, 1985: Spectral characteristicals of P wave from nuclear explosions and yield estimation. *Bull. Seism. Soc. Am.*, **75**, 379-390.

Hanks, T. C., 1979: b-value and $\omega^{-\alpha}$ seismic source models: implications for tectonic stress variations along active crustal fault zones and the estimation of high-frequency strong ground motion. *J. Geophys. Res.*, **84**, 2235-2242.

Hough, S. E., J. G. Anderson, J. Brune, F. Vernon, III, J. Berger, J. Fletcher, L. Harr, T. Hanks, and L. Baker, 1988: Attenuation near Anza, California. *Bull. Seism. Soc. Am.*, **78**, 672-691.

Hough, S. E., and J. G. Anderson, 1988: High-frequency spectra observed at Anza, California: implications for Q structure. *Bull. Seism. Soc. Am.*, **78**, 692-707.

Kanamori, H., 1967a: Spectrum of short-period core phases in relation to the attenuation in the mantle. *J. Geophys. Res.*, **72**, 2181-2186.

Kanamori, H., 1967b: Spectrum of P and PcP in relation to the mantle-core boundary and attenuation in the mantle. *J. Geophys. Res.*, **72**, 559-571.

Kanamori, H., and D. L. Anderson, 1977: Importance of dispersion in surface wave and free oscillation problems: Review. *Rev. Gephys. Space Phys.*, **15** 105-112.

Knopoff, L., 1964: Q. *Rev. Geophys.*, **2**, 625-660.

Lee, W. B., and S. C. Solomon, 1978: Simultaneous inversion of surface wave phase velocity and attenuation: Love waves in Western North America. *J. Geophys. Res.*, **83**, 3389-3400.

Letouzey, J., and M. Kimura, 1986: The Okinawa Trough : genesis of a back-arc basin developing along a continental margin. *Tectonophysics*, **125**, 209-230.

Lundquist, G. M., and V. C. Cormier, 1980: Constraints on the absorption model of Q. *J. Geophys. Res.*, **85**, 5244-5266.

Mitchell, B. J., 1980: Frequency dependence of shear wave internal fricton in the continental crust of eastern North America. *J. Geophys. Res.*, **85**, 5212-5218.

Mitchell, B. J., 1981: Regional variance and frequency dependence of Qb in the crust of the United States. *Bull. Seism. Soc. Am.*, **71**, 1531-1538.

Modiano, T., and D. Hatzfeld, 1982: Experimental study of the spectral content for shallow earthquakes. *Bull. Seism. Soc. Am.*, **72**, 1739-1758.

Roecker, S. W., Y. H. Yeh, and Y. B. Tsai, 1987: Three-dimensional P and S wave velocity structures beneath Taiwan: Deep structure beneath an arc-continental collision. *J. Geophys. Res.*, **92**, 10547-10570.

Seno, T., 1977: The instantaneous rotation vector of the Philippine Sea plate relative to the Eurasian plate. *Tectonophysics*, **42**, 209-226.

Solomon, S. C., 1972: Seismic wave attenuation and partial melting in the upper mantle of North America. *J. Geophys. Res.*, **77**, 1483-1502.

Solomon, S. C., 1973: Shear wave attenuation and melting beneath the mid-Atlantic ridge. *J. Geophys. Res.*, **78**, 6044-6059.

Teng, T. L., 1968: An attenuation of body waves and the Q structure of the mantle. *J. Geophys. Res.*, **73**, 2195-2208.

Thurber, C. H., and W. L., Ellsworth, 1980: Rapid solution of ray tracing problems in heterogeneous media. *Bull. Seism. Soc. Am.*, **70**, 1137-1148.

Yeh, Y. H., E. Darrier, C. H. Lin, and J. Anglier, 1991: Stress tensor analysis in the Taiwan area from focal mechanisms. *Tectonogphsics*, **200**, 267-280.